ENGINEERING TRANSACTIONS • *Engng. Trans.* • **49**, 4, 599–621, 2001
Polish Academy of Sciences • Institute of Fundamental Technological Research
10.24423/engtrans.544.2001

ON THE EFFICIENCY OF THE SOIL DIGGING PROCESSES

J. MACIEJEWSKI[1], A. JARZĘBOWSKI[1]
and
W. TRĄMPCZYŃSKI[2]

[1]**Institute of Fundamental Technological Research**
Polish Academy of Sciences, Warsaw, Poland

[2]**Department of Civil Engineering,**
Technical University of Kielce, Poland

In the first part of the paper, an experimental verification of correctness of the common assumption that the plane strain conditions occur in the tests performed in soil bins is presented. An experimental program was executed basing on the soil cutting problem, with the application of vertical rigid walls of various widths as the working tools. It turned out that in the case of the tool width equal to the width of the soil bin, the soil cutting problems may be treated as the plane strain processes. The influence of the friction phenomena on the side walls of the bin was estimated. For the tools for which no interaction with the side walls of the bin was observed, the zone of the plane strain deformation occurred in the central part of the tools. Then the characteristic deformation patterns and force-displacement relations for the L-shaped tool are determined. Finally, the new idea of the optimization of digging be means of the earth-working machinery is presented and experimentally verified. Dividing the whole excavation task into several repeatable cycles for which the soil free boundary before and after the experiment are similar, the optimization of the single cycle plays a significant role in the energetic efficiency of the whole task. The single cycle of the working process is defined using several basic parameters. The influence of each parameter on the specific unit energy of the process is experimentally verified. The set of values of the discussed parameters is recommended for the particular soil and tool shape. The disadvantages of other soil cutting strategies are discussed.

1. Introduction

Since the first automatic excavator FUTURE was presented on the BAUMA exhibition in 1983, various attempts were made by producers to develop automation systems. The role of the widest group of such systems is to assist an operator in his work by "on line" monitoring of the actual state of the machine, continuous monitoring of the bucket position and weight, controlling of the machine stability and various "teach-in" systems.

However, relatively little was done to develop an intelligent system of automatic digging, which would react to the actual state of the soil and allow for the reduction of the loss during the earth-working process. One may conclude that the most important phase of the excavator working cycle – the digging itself – has not been automated or even optimised until now. The aim of this paper is to develop some useful ideas of such an optimisation.

During the cohesive soil-rigid tool interaction process a characteristic deformation pattern consisting of several rigid blocks separated by shear bands is observed [1–10]. This phenomenon is correlated with the material softening occurring within the zone of the shear bands and local degradation of material's parameters, as well as the global drop of the force acting on the rigid tool. During progressive motion of the tool the initial failure mechanism is modifying. Some of shear bands are material planes, while remaining bands move with respect to the material in order to constitute a kinematically admissible failure mode. A characteristic effect of switching to new failure modes occurs at particular states of the deformation process, resulting in an oscillatory force-displacement response.

The phenomenon of slip line generation becomes the most important factor for the optimisation of the soil cutting process combined with the machine tool filling process. The idea of such a machine tool control to displace the tip of the tool along the previously generated slip line was introduced and developed in papers [7–10]. The specific energy for the soil excavating process depends on several parameters, among which the most important are: the material behaviour (softening), the tool shape, the tool trajectory and the free boundary configuration of the excavated material.

When the earth moving processes due to the motion of heavy machinery tool are considered, quite often the plane strain condition occurs. In practical cases, when the motion of an excavator bucket, a loader bucket or a bulldozer blade is discussed, the plane strain conditions are fulfilled only in some deformation regions. Hence, the plane strain solutions for such tools can be assumed only with certain accuracy.

Experimental verification of earth-moving processes is usually carried out in a soil bin as a movement of a model tool between two transparent walls [1–11]. The correctness of the common assumption that the plane strain conditions occur for the tests performed in soil bins is the subject of the first part of this paper. The soil deformation, observed through transparent walls and the force acting on the tool are registered during the process and then compared with theoretical predictions [3,6,7]. For such measurements, the influence of side walls on the soil deformation and on the force acting on the tool due to the friction between the soil and side walls has to be estimated or neglected.

2. Experimental procedure

All experiments were performed in a semi-laboratory scale using the special computer-controlled stand (Fig. 1a) [7–9]. The soil sample was prepared in a fixed container ($2 \times 1.2 \times 0.6$ [m]) having one transparent wall to enable photographic recording of the material in motion. The tested model of the tool (1) was moved within the container by means of three hydraulic jacks, the motion of which was computer-controlled through the electric proportional valves and a hydraulic pump. The set of loading cells (2) mounted on the rigid frame (3) allowed for the measurement of all force components acting on the tool within the range of +/− 10000 N, with the accuracy of 4 N.

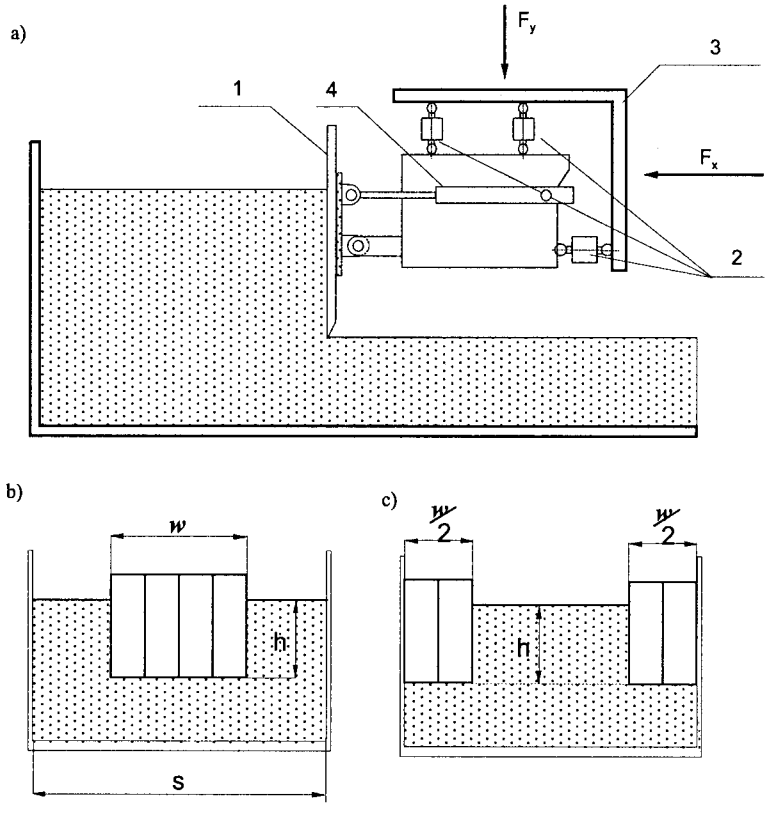

Fig. 1. Scheme of experimental program; a) side view of the soil bin, b) tools used in the first series of tests, c) tools used in the second series of tests.

The displacement of the tool was measured by two linear extensometers and a rotational one. All data obtained this way was analysed (and stored) by the computer and used for the "on line" control.

The special artificial material, imitating clay and its parameters, was used for the experiments. It consisted of cement −50%, bentonite −20%, sand −18% and white vaseline −12%. All components were heated in a furnace, mixed and cooled to the room temperature. Application of white vaseline, as one of the components, resulted in obtaining a cohesive soil of parameters which were not influenced by air humidity and liquid flow. It also ensured that those parameters were stable during the whole experimental program. However, it was observed that the soil model was sensitive to seasonal changes of temperature in the laboratory (summer – winter). Hence, only the tests results during the same season were compared.

The soil sample was prepared in the soil bin layer by layer. The compaction of each layer was obtained by means of a rigid stamp, covering the free surface during several passes. The pressure exerted by the stamp controlled by the computer was adjusted to ensure homogeneity of the soil sample. Then, the vertical front rigid wall of the soil bin was removed and a scarp obeying horizontal free surface was obtained. The soil sample prepared according to this procedure can be described by the Coulomb-Mohr model with the following parameters: specific density $\gamma = 18.4$ kN/m^3, internal friction angle $\rho = 24°$ and cohesion $c = \sim 20$ kPa, what corresponds to sandy clay. During the deformation process, the soil changed its parameters due to material softening (especially the decrease of cohesion was observed).

3. Experimental results for the walls of different widths

In the first series of the tests, a set of vertical rigid walls of six different widths w : 65, 130, 195, 260, 325 and 390 mm, situated centrally in the soil bin (Fig. 1b) was moved horizontally. The working depth *"h"* was equal to 100 mm and horizontal tool displacement was equal to 400 mm for each test executed within both series of the experiments. For the wall of 65 mm width, quite complicated three-dimensional soil deformation pattern was observed (Fig. 2a). However, while increasing the width of the tool ($w > 130$ mm), one could distinguish the central part of the dump, parallel to the surface of the wall, where plane strain condition was realised, and two zones where side dumps of three-dimensional pattern were generated. It is schematically presented in Fig. 2 as a top view. Starting from the tool width $w = 130$ mm, the width of the front dump was increasing (plane strain region – Fig. 2b – DCGF), whereas the shape of the side dumps (Fig. 2b – ADFE and CBHG) was similar for each test and did not depend on the width of the wall. The width of the plane strain region was smaller than the tool width (Fig. 2b – AB and DC) but it increased when the tool width was increasing. For the tool widths $w = 65$, 130, 195, 260, the generation of side parts of dump was

not influenced by the side walls limiting the soil bin. However, for the widest tools (325 and 390 mm), such influence was observed (Fig. 2c).

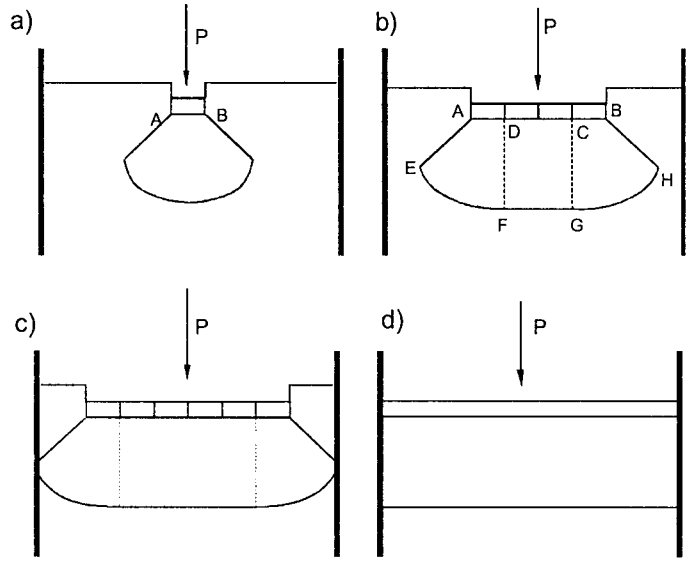

FIG. 2. Top view of dumps for different widths of centrally situated tool.

The cyclic repeatability of the process was observed with the developing horizontal displacement of the tool. The deformation pattern consisted of several rigid blocks sliding on the shear bands where material softening was observed. As a consequence, reduction of the horizontal force and abrupt changes of the deformation mechanisms were noticed. Precise description of this soil-tool interaction was given in [6–9]. The results of the horizontal force variation for each of the six centrally situated rigid walls is plotted in Fig. 3 for 400 mm displacement of the tool. The result for horizontal movement of the vertical rigid wall of the width equal to that of the soil bin (Fig. 2d) is additionally plotted in that figure.

In the second series of experiments two rigid walls situated symmetrically – neighbouring the side walls – were used (Fig. 1c). Similarly to the first series, three different widths $w/2$ of each wall were used: 65, 130 and 195 mm, resulting in the total width of working tool equal to 130, 260 and 390 mm (Fig. 1) (the width of the left and right-hand walls were equal during each test).

When the tool started to move, two symmetrical dumps were generated (Fig. 4a – BCDE and GHKL). It is schematically presented in Fig. 4a as a top view. The shape and range of these side dumps were identical to the side dumps

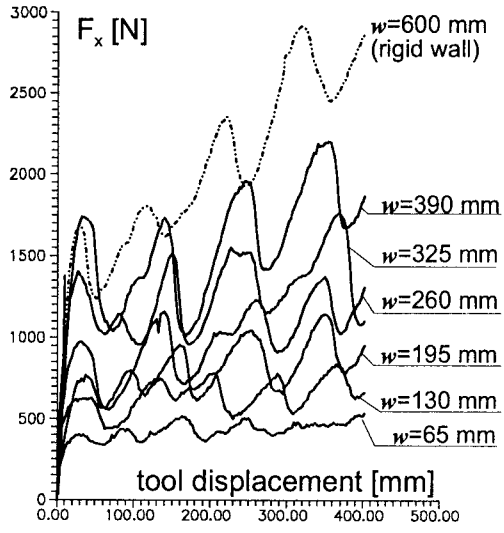

FIG. 3. Horizontal force variation for six different widths of centrally situated rigid walls.

generated during the corresponding experiments of the first series (Fig. 2b – ADFE and CBHG). For the tools 130 and 195 mm wide, the front dump parallel to the surface of the wall was observed (Fig. 4a – ABEF and HIJK) between the side dumps and the side wall of the bin. The plane strain conditions were realised in these regions. As in the first series of the tests, the width of the plane strain region was smaller than the tool width (Fig. 4a – compare AC and AB, GI and HI), but it increased when the tool width was increasing. No interaction between the side dumps was noticed for 65 and 130 mm rigid walls. However, for the walls of 195 mm width (total width 390 mm), the bilateral influence between the dumps was observed (Fig. 4b).

It is worth to compare the side deformation patterns for the rigid wall (Fig. 5a) and the side walls of 65 mm width (Fig. 5b). As the process develops, one may easily distinguish the same range of deformation zones and the corresponding slip lines occurring in Fig. 5a and 5b, what suggests that the deformation patterns are similar for the tools of different widths.

The results of the horizontal force variation for tools neighbouring the side walls of the soil bin are presented in Fig. 6 for 400 mm tool displacement. The result for vertical rigid wall of width equal to that of the soil bin (Fig. 2d) is also plotted in that figure.

On the basis of the results presented in Figs. 3 and 6, the first peak values of horizontal force were plotted in Fig. 7 using squares and dots for the first and the second series of the tests, respectively, and x-mark for the rigid wall test. Mean

values taken from several identical tests were used to prepare Fig. 7. Since the deformation was not ideal rigid-perfectly plastic, the total work generated by the external horizontal force over the distance of 50 mm (horizontal tool displacement corresponding to the first drop of the horizontal force) was calculated for both series of experiments. The obtained values of the work integrals are plotted in Fig. 8.

The relation between the peak values of the horizontal force and the tool width for the first series of experiments (centrally situated wall – squares) is linear for tool widths from the range of 130 to 260 mm (Fig. 7 – dashed line). Starting from the tool width 130 mm, the plane strain region in the tool centre begins to form and subsequently grows when the tool width increases. For widths over 300 mm, the interaction of side dumps with side walls makes the horizontal force reach higher values than it follows from the above-described linear relation. For tool widths 65 and 130 mm, only the three-dimensional dumps were observed in front of the tools (without linear zone). Thus, it was assumed that the whole force for those tools was necessary to generate the side dumps only. It was noticed basing on the photographic recording of experiments that, using the tools widths equal and greater than 130 mm, the three-dimensional side dumps were well developed and did not change their shape and range. Thus, it was assumed that the force necessary for generation of the side dumps did not change from 130 mm tool width (solid and dashed horizontal line).

For tool widths 130 and 190 mm, the only difference between both series of experiments is caused by friction between the soil and the side walls (Fig. 2b and Fig. 4a). Hence, the distance between the corresponding experiments (marked by triangles in Fig. 7) denotes the value of the friction force component during the process. It was assumed that the friction force component does not depend on the tool width (horizontal dotted line). Knowing the value of the horizontal force in the case of vertical rigid wall of width equal to the soil bin (Fig. 7 – tool width 600 mm, x-mark), the plane strain force contribution can be calculated

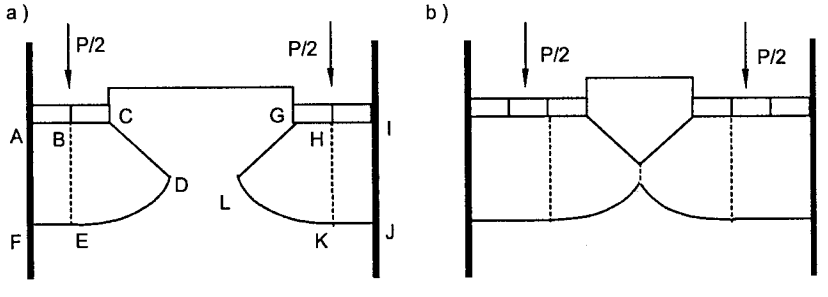

FIG. 4. Top view of dumps for different widths of tool for the second series of tests.

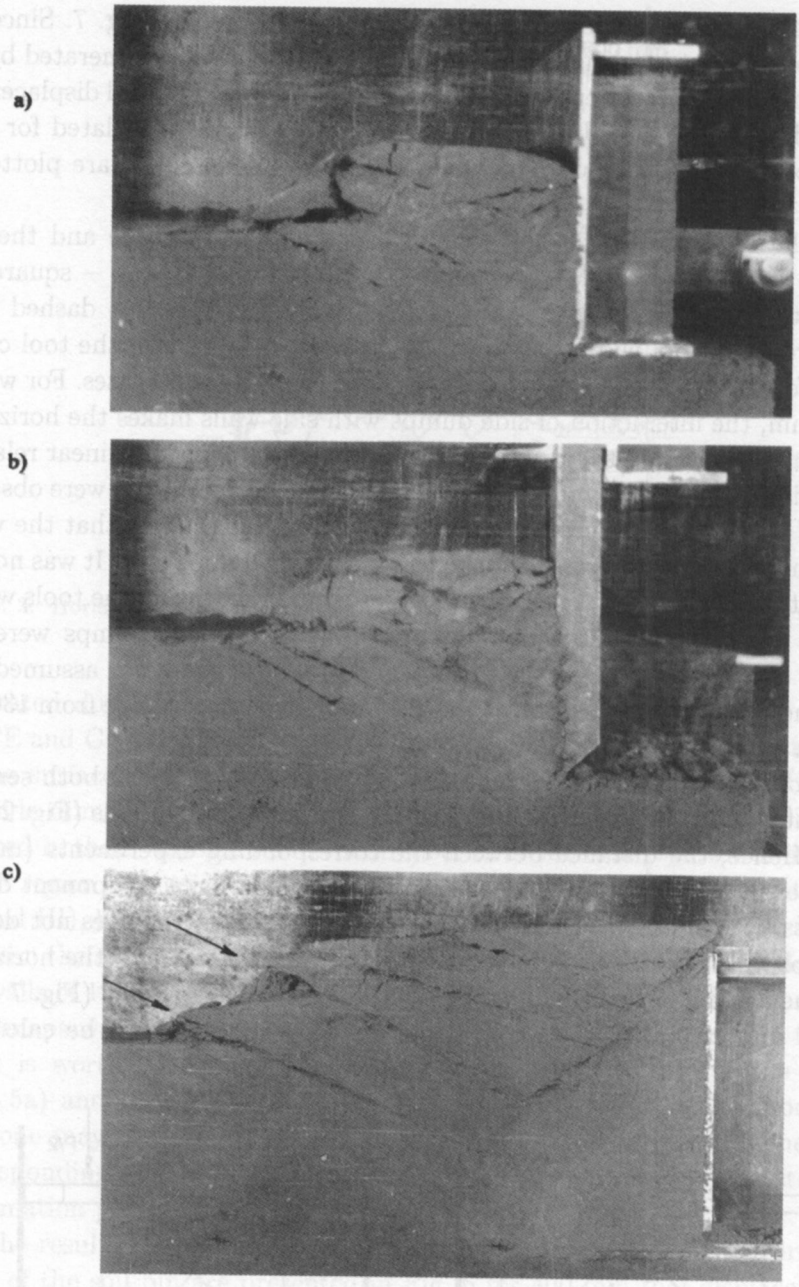

FIG. 5. Deformation patterns during the pushing processes; a) rigid wall of 600 mm width, b) side wall of 65 mm width, c) "L"- shaped tool of 600 mm width.

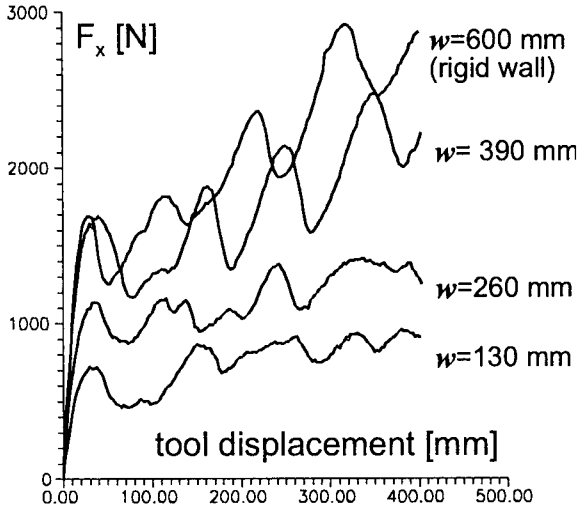

FIG. 6. Horizontal force variation for different widths of tool for the second series of tests.

(Fig. 7 – x-mark). It turned out that for particular tool proportions, the friction force component is about $\sim$ 10% of the total force.

It means that when plane strain experiments were carried out in the soil bin described, the force component of the plane strain process (for the tool dimensions mentioned above) was close to 90% of the total force. Basing on those results, the force component of the plane strain process per unit width of the plane strain region may be calculated as the inclination of the thin dashed line plotted in Fig. 7. However, the lateral component of the stress state within the plane strain region for the tools with three-dimensional side dumps had probably slightly higher value than the stress state for the tools of width equal to the soil bin width (rigid wall tests). It explains the difference between the inclination of thin and thick dashed lines (Fig. 7) denoting the force of the plane strain process per unit width of the plane strain region for rigid wall tool and tools of variable width. Magnitude of this difference (8% in case of our experiments) means that all tests realised by tools of width equal to the soil bin may be treated as the plane strain tests with satisfactory accuracy.

Similar results were obtained for the work generated by the external horizontal force over the distance of 50 mm (Fig. 8).

As a result of the described program of laboratory tests (for the given cohesive soil, tool proportions and tools acting in the earth-pushing working regime), the following conclusions may be derived:

- The zone of plane strain process generates within the central part of the tool for tools which are wide enough (for the presented experiments it was

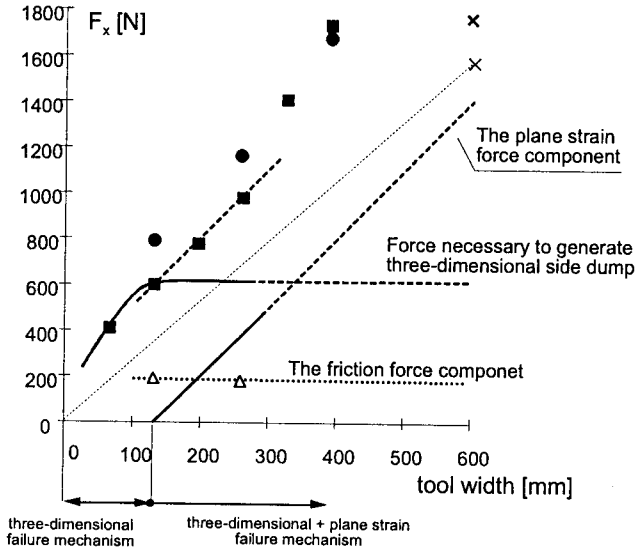

FIG. 7. Force values for the first peak of horizontal force.

$>$ 130 mm for 100 mm depth of soil cutting). The character of the plane strain process is the same, independently of the type of the test (centrally situated wide tool, two rigid side walls).

- For centrally situated wall tool of 320 mm width, the plane strain energy is about 50 % of the total energy of the process. For predicted width of the tool 1000 mm (10 times greater than the cutting depth in our case), the contribution of plane strain energy will be equal to 80% of the total energy.
- Thus, the plane strain part of the process plays an important role in soil cutting processes, even for tools which are not commonly treated as "wide". However, even for so-called "wide tools", the energy of side dumps generation has to be taken into account.
- All tests performed using rigid wall of width equal to the width of the soil bin may be treated as plane strain tests. The friction on the side walls does not influence the deformation patterns from the qualitative point of view. The contribution of friction energy was close to 10% of the total energy. The difference between plane strain energy for the rigid wall tests and the tests for tools of variable width may be neglected with sufficient accuracy.
- While performing the tests in soil bins one must be very careful to avoid the interaction between the side dumps and the side walls. In the case of described tests (tool height to soil bin width ratio equal to 1/6), that interaction started for tool widths greater than 50% of the soil bin width.

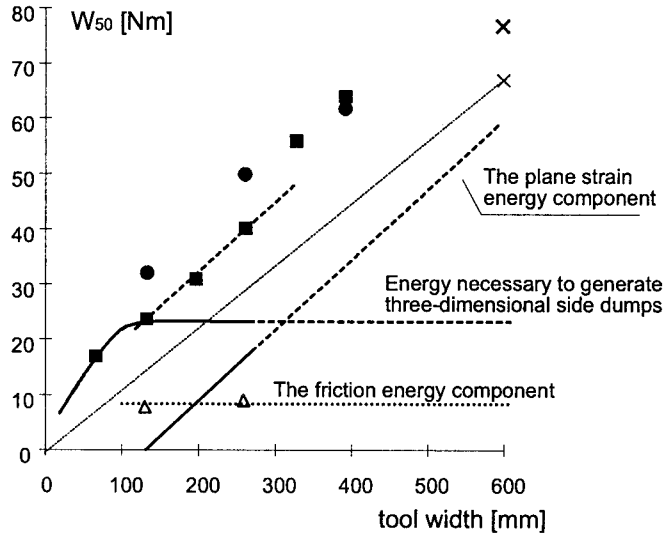

FIG. 8. Calculated work integrals over the distance of 50 mm horizontal tool displacement.

4. EXPERIMENTAL RESULTS FOR THE "L" - SHAPED MODEL TOOL

The described above phenomenon of slip line generation was later applied in the process of searching for the most efficient soil cutting and tool filling trajectory. Using the described above stand it was possible to simulate a wide program of soil shoving processes with different working paths. In that series of experiments, the L-shaped model tool was applied. Since the tool had the width equal to the width of the soil container, all tests were approximately performed under plane strain conditions.

During each test the tool was subjected to horizontal motion (with the tool inclination $\delta = 5°$) and, consequently, it initially penetrated the soil sample and later it pushed the sample by its rear wall. As a result, similarly to the rigid wall tests, the characteristic soil deformation pattern was observed, consisting of several rigid zones sliding along the slip lines (Fig. 5c). This phenomenon resulted in an unstable relation between the horizontal component of the earth working force and the tool displacement as the process advanced. In Fig. 9 the horizontal force component versus horizontal displacement is presented. The initial stage of the sample penetration can easily be distinguished by slight increase of horizontal force component (cf. Fig. 9 line Z). When the rear wall of the L-shaped tool gets in contact with the sample, the force rapidly increases (the increase of 400%). From this moment on, the instant of the force drop coincided with the creation of a new slip line originating from the tip of the tool. Creation of the slip lines

repeated periodically, similarly to the rigid wall pushing tests described in the previous part of this paper.

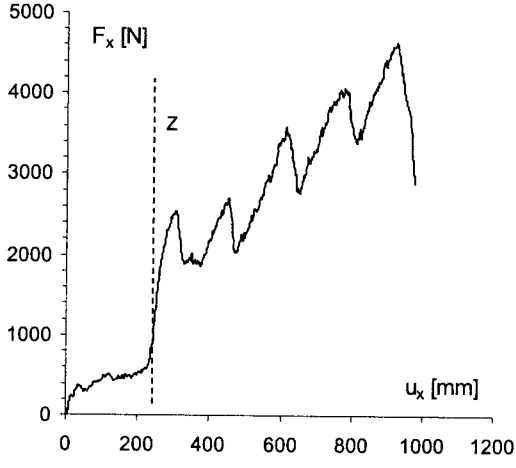

FIG. 9. Horizontal force versus horizontal displacement during the pushing process for the "L"-shaped tool.

The simplest idea for optimisation of the earth-working process was to follow the tip of the tool along the slip line generated in the pushing phase of the process. To verify this idea, a set of tests was performed on the model soil samples with horizontal boundaries. Each experiment was performed in two stages. During the first stage the model tool (inclined at an angle of 5° degrees to avoid friction between the bottom of the tool and the remaining layer of soil) was pushed horizontally through the soil sample. In the second stage, the tool was "withdrawn" from the sample by parallel translation along the straight lines with various inclinations (Fig. 10a).

In that group of experiments the same first phase of the process was executed, and in the second phase the path inclinations of 20°, 31° and 42° degrees were used. The value of 31ř degrees was equal to the inclination of the slip lines generated during the first stage of the process.

The amount of specific energy W_f calculated for the unit weight of the soil excavated was computed for every test to allow direct comparison. In Fig. 10b the relation between the horizontal force and the displacement of the tool is presented for the three trajectories mentioned above, whereas in Fig. 10c the relation between specific energy W_f and trajectory inclination is plotted. Although the amount of the soil excavated increased with decreasing trajectory inclinations, the efficiency of the process was also decreasing (notice high value

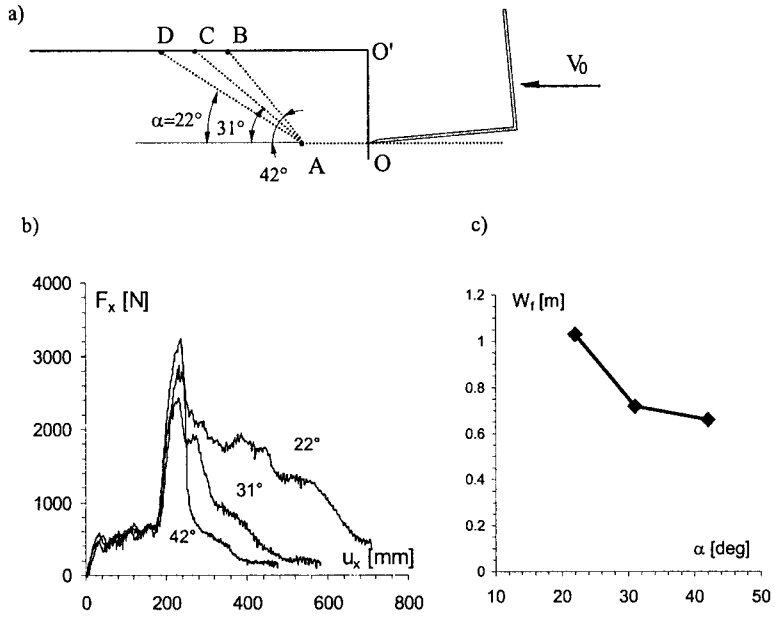

FIG. 10. Experimental results for digging process: a) scheme of the tests, b) horizontal force versus horizontal displacement for three different trajectory inclinations, c) values of specific work W_f versus trajectory inclinations.

of energy for the inclination of 22° degrees). It was caused by generation of new slip lines even during the "withdrawing" phase. The efficiency of trajectories with inclination similar or higher than the inclination of the naturally generated slip line was comparable in both the cases (the difference in specific energy was equal to 10%).

The optimisation of the soil cutting and the machine tool filling process was later investigated [7–9] basing on the single cycle of the earth-working equipment executed on the initially prescribed slope of the sample. The slope of the assumed inclination was prepared before each test resulting in the constant initial condition. The influence of several parameters on the efficiency of the earth-working process was investigated. They were the shape of the tool trajectory, the shape of the cross-section of the bucket and the inclination of the withdraw trajectory phase.

It was concluded that, conducting the tool tip along the line inclined at the angle similar to the angle of slip lines inclinations, the specific energy of the earth-filling process can be significantly reduced for the single work cycle.

Experimental results proved that the specific unit energy had the lowest value for the "long" bottom tool. In such a case, the pushing effect of the tool's back

wall was not observed. It means that analysing the tool filling process using the reduction of the specific unit energy as the major optimisation criterion, the most favourable tool shapes are obtained when the energy due to the tool back wall pushing process is minimised.

The above-mentioned results were obtained for the sets of single earth working processes consisting of the tool penetration along the curvilinear or piece-wise linear trajectory, and the tool withdrawal phases executed on the initially prepared slope sample. For this reason, the soil configurations before and after the test were different.

5. Optimisation of repeatable tool trajectory

Basing on the conclusions that there are optimal soil cutting trajectories in laboratory conditions [8,9], a new experimental program was launched for repeatable tests, for which the soil free boundaries before and after the experiment were similar. Assuming that the whole excavation task consists of several repeatable cycles (Fig. 11), the optimisation of the single cycle plays a significant role in the energetical efficiency of the whole earth-working task. In this experimental program, the simplified model of the K-111 Waryński excavator bucket without teeth was used.

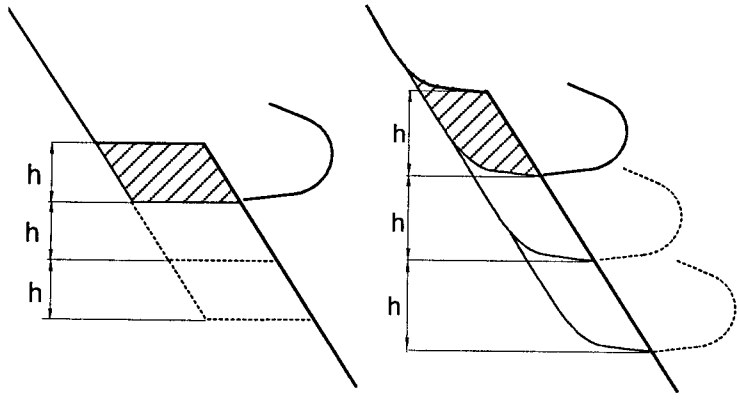

Fig. 11. Scheme of the repeatable cycles of digging process.

All tests were performed on the same stand and the same modelling material, which were described in the previous chapter. The initial configuration of the soil sample (slope) was shaped in several repeatable movements of the bucket.

During each test, the force acting on the tool was measured and recorded and the total work W was calculated after each experiment. To allow a direct

comparison of results obtained for various tests, the total work W was corrected according to the initial position of the mass centre of the volume dug out:

$$W_c = W - (y_c - y_i)Q, \tag{5.1}$$

where W_c is the corrected value of the total work of the process, Q is the weight of the material which remained in the bucket, and y_i and y_c denote the vertical components of the positions of the mass centres of the material dug out in the initial and the final moment of the process, respectively.

As it was experimentally proved, that the energetic efficiency of the curvilinear trajectories and of the corresponding piece-wise linear trajectories is similar, only various piece-linear trajectories were used in this experimental program.

Typical piece-wise linear trajectories for which soil configurations before and after each test were equal are presented in Fig. 12. To describe the single cycle of the working process, the following parameters were used:

α – the slope inclination (equal to the inclination of the withdraw phase),
β – the inclination of the initial phase of trajectory,
δ – the tool inclination,
h – height of the excavated material,
b – width of the excavated material.

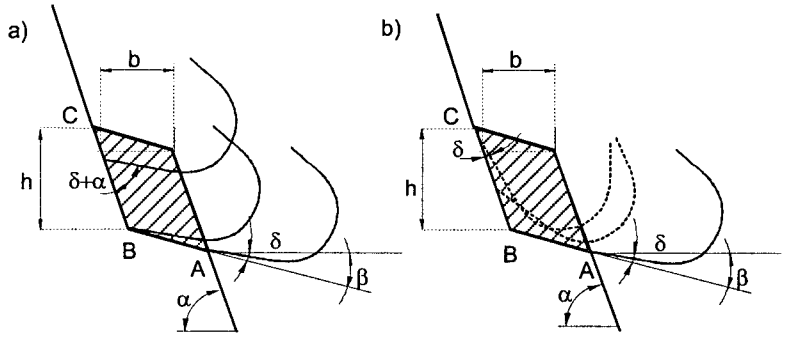

FIG. 12. Scheme of the single cycle and its parameters; a) translatory tool motion, b) combined tool motion.

For each experimental cycle of the working process for which the bucket moves with the combination of translation and rotational components (Fig. 13), several characteristic phases may be distinguished. At the initial phase of the movement, the translation displacement of the tool along the straight line AB was executed. During this phase the soil started to fill the bucket, and the characteristic deformation pattern, typical for materials obeying softening, consisting

of several rigid blocks separated by slip lines, appeared. The deformation zone was limited to the area located above the tool and did not propagate into the virgin material prior to the assumed tool trajectory.

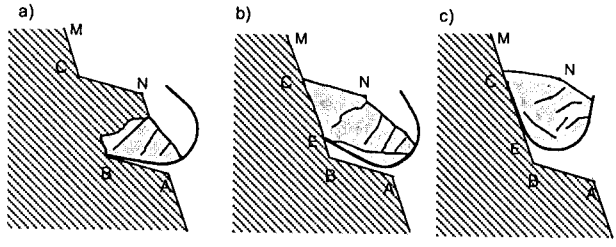

FIG. 13. Subsequent phases of the single cycle of digging process.

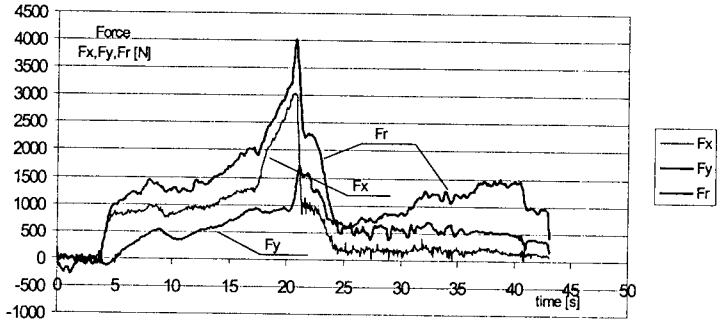

FIG. 14. Typical force-time diagram.

An example of the development of the horizontal force versus horizontal displacement of the tool for the cross-section area of the dug-out material equal to ~42000 mm^2 is presented in Fig. 14. For the horizontal displacement greater than the displacement corresponding to the complete fulfilment of the bucket, the significant increase of the force caused by strong reaction of the soil on the tool rear wall was observed (the developed pushing process).

At the point B, the second phase of the trajectory was executed. The tool changed its direction passing to the withdrawal phase. During the change of the direction of the tool motion, the slip line BEC (Fig. 13b) was created. It is worth to point out that the slip line generated from the point B to the point C (which was the corner point of the free boundary MCN), independently of the slope inclination, as well, as other parameters of the working cycle. The inclination of the new generated slip line BEC was close to the slope inclination.

In the final phase of the trajectory (Fig. 13c), the translation of the bucket was performed to displace the tip of the tool along the slip line EC and proceed to the point M.

In the initial series of tests, each working cycle was executed using two different approaches: rigid translation of the tool and translation combined with rotation. In the case of translation trajectories, the value of the tool inclination angle δ abruptly increased at the point B to the value of $\delta + \alpha$ (Fig. 12a). It resulted in significant growth of the specific unit energy of the process caused by the abrupt increase of the earth-working force and raise on the bucket filling resistance.

In the case of trajectories during which the translation of the tool was combined with its rotation to ensure constant value of the tool inclination δ, the specific unit energy of the process was lower. In the case of trajectories with constant tool inclination δ, the geometrical parameters of the tool and the trajectory were taken into account, ensuring that there were no collisions between the bottom of the bucket and the virgin slope.

Results of the set of tests investigating the influence of the tool inclination angle δ on the specific unit energy of the process are presented in Fig. 15. This group of experiments was executed on the soil sample with the slope inclination of 50°, keeping constant ratio of the parameters b : h equal to 150 : 220 [mm]. Such a cross-section of the side area of the material dug-out corresponded to the area of the cross-section of the bucket.

In the case of combined trajectory (translation + rotation of the bucket), no significant influence of the tool inclination angle δ on the specific unit energy was noticed within the investigated range of that angle (5°, 15°, 30°). However, in the case of pure translation trajectory (with no rotation), the specific unit energy increases by over 40% for the change of d from 5° to 15°. For further change of δ (from 15° to 30°), a slight raise of the specific unit energy was observed (Fig. 15).

The influence of the inclination β of the trajectory initial part on the specific unit energy of the process was investigated for the slope inclination equal to 70° and constant ratio of the parameters b : h equal to 150 : 220 [mm] (as in the previous set of tests). The scheme of trajectories used in this set of tests and the results are presented in Fig. 16. The lowest value of the specific energy was obtained for the horizontal initial part of the trajectory ($\beta = 0°$).

From the subsequent series of experiments, only the tests performed with the horizontal initial part of the trajectory ($\beta = 0°$) and the angle of tool inclination $\delta = 5°$ were selected for combined trajectories (translation with rotation of the bucket). The influence of the two major parameters was investigated: the volume of the dug-out material with constant ratio b : h and the ratio b : h with constant volume V. Two different values of the slope inclination were used: $\alpha = 50°$ and $\alpha = 70°$.

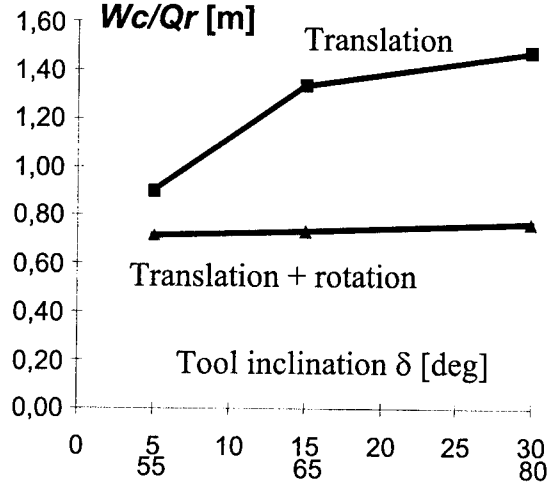

FIG. 15. Values of specific energy versus the angle of tool inclination for different tool motions.

The influence of the slope inclination was investigated for two different ratios b : h (110 : 300 and 150 : 220 [mm]) and constant volume of the excavated material. Various slope inclinations within the range from 30° to 85° were used and the test results are presented in Fig. 17. The most efficient results were obtained for the slope inclination of 70°. For higher values of slope inclination, the energy of the process increases due to harmful development of soil pushing phase. On the other hand, for lower slope inclinations the length of the slip lines was increasing resulting in higher energy consumption. The execution of the test for the ratio b : h equal to 110 : 300 [mm] turned out to be impossible for the slope inclination of 85° due to kinematic reasons (the top part of the bucket hit the slope before the end of the first phase of the tool trajectory).

Results of tests for different area of the cross-section of the dug-out material are presented in Fig. 18. The existence of the optimal volume was observed for both slope inclinations. This volume corresponded to the volume of the bucket. In addition, for greater volumes of the excavated material some amount of the material was falling out from the bucket, resulting in significant rise of the specific unit energy (Fig. 18b).

In Fig. 19 the results of tests performed for constant volume of the dug-out material are presented. The influence of the ratio b : h on the specific unit energy of the process was investigated. As previously, the existence of the optimal value of the ratio b : h was observed for the ratio b : h equal to 150 : 220 [mm]. In

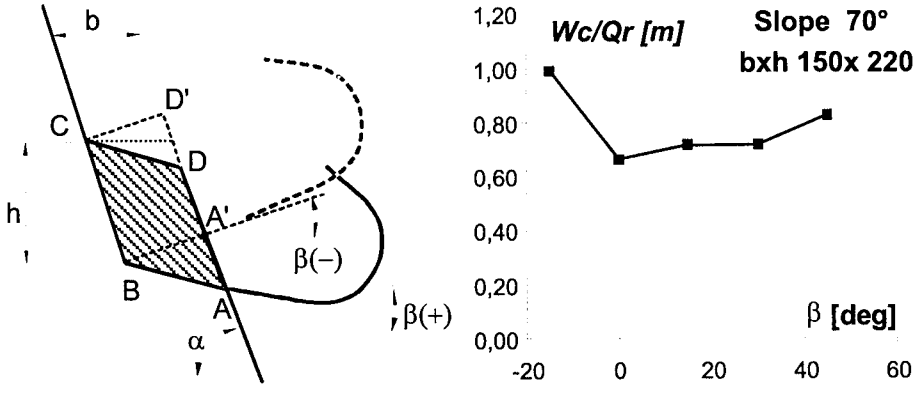

FIG. 16. Values of specific energy versus the angle of inclination of the initial phase of trajectory.

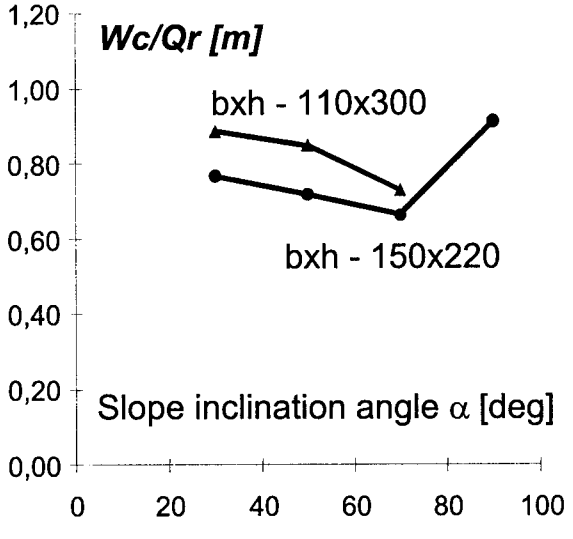

FIG. 17. Values of specific energy versus the angle of slope inclination.

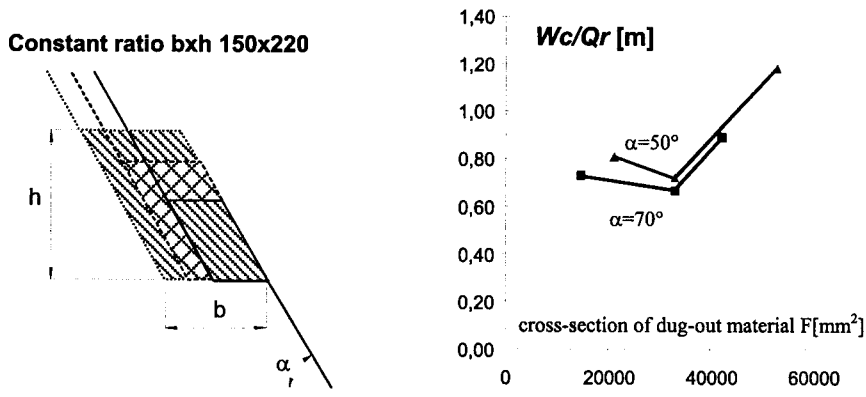

FIG. 18. Values of specific energy versus the area of the cross-section of dug-out material and constant b : h ratio.

addition, the maximal values of each force (peak values) exerted by hydraulic jacks responsible for the horizontal, vertical and rotational motion of the tool for different values of the ratio b : h, are plotted in Fig. 20. Although those maximal values of forces occurred in different moments of the processes, the optimal value of all three components was observed for the same ratio b : h equal to 150 : 220.

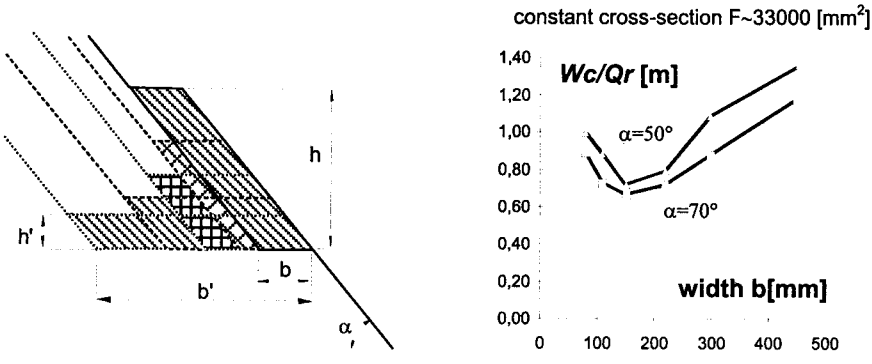

FIG. 19. Values of specific energy versus different b : h ratio and constant volume of dug-out material.

It was shown that the soil cutting strategy basing on cutting of a thin layer horizontally or vertically was not reasonable (Fig. 19a). Neither the specific unit energy nor the exerted forces were optimal for this method of soil cutting. It was caused by continuous earth pressure exerted by the soil layer on the rear wall of the tool during the tool filling process (Fig. 21).

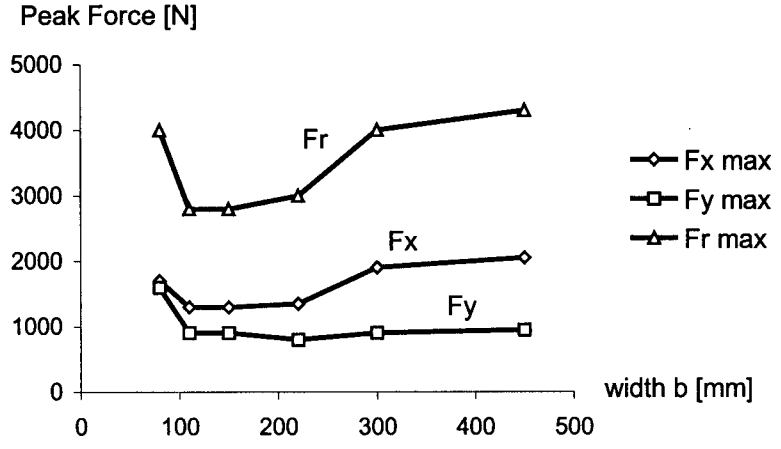

FIG. 20. Diagram of peak force components versus width b ratio for constant volume of dug-out material.

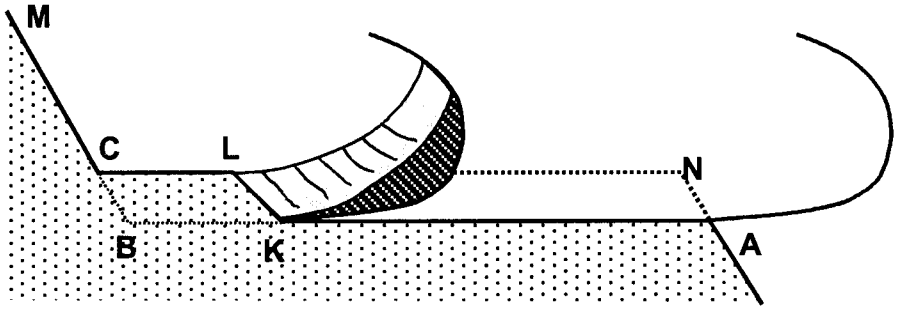

FIG. 21. Scheme of the digging process for thin soil layer.

6. Concluding remarks

Periodic character of the earth-working process (observed for the cohesive soil with softening) manifested in the oscillatory character of force components and generation of the subsequent slip lines is independent of the width of the tool and the shape of the free boundary surface.

As it was proved in previous papers [7–9], the optimisation of any single earth-working cycle of the bucket equipped machine is possible basing on the idea of incorporating the generated slip line as a part of the tool trajectory.

However, the difference of the shapes of the soil free surfaces before and after the cycle results in the necessity of independent optimisation of each subsequent cycle. For this reason, an attempt of optimisation of the earth-working task consisting of repeated single cycles was presented in the second part of this paper. Such an optimisation may be useful in the excavation task performed by the automatically controlled excavator, allowing for ensuring constant cycle parameters independently of the operator. It is worth to point out that only the combination of digging and bucket filling phases were considered in this paper, excluding the influence of the kinematics of the whole equipment (the bucket, the arm and the boom motion) on the energy consumption.

It was found that for the particular soil and the model of the tool used in this study, the following parameters of the single cycle executed as the combination of translation and rotation, turned out to be most efficient: $\alpha = 70°$, $\beta = 0°$, $\delta = 5°$, $h = 220$ mm, $b = 150$ mm. The values of h and b correspond to the cross-sectional area of the bucket.

It turned out that the soil digging method recommended by some authors, basing on cutting thin layers of material turned out to be inefficient. Such a strategy results in continuous cutting of the material, generating several subsequent slip lines and exerting continuous earth pressure on the rear wall of the tool during the tool filling process. Consequently, the specific energy dissipation per unit volume of the dug out material is higher compared with other digging strategies. In addition, contrary to the common approaches, the exerted forces are higher due to necessity of continuous pushing of the material layers during the tool-filling phase.

References

1. R. Butterfield, K. Z. Andrawes, *An investigation of a plane strain continuous penetration problem*, Geotechnique **22**, 4, 597-617, 1972.

2. Y. Hatamura, K. Chijiiwa, *Analysis of the mechanism of soil cutting*, Bulletin of the JSME, **18**, 120, 1975; **19**, 131, 1976; **19**, 137, 1976; **20**, 139, 1977; **20**, 141, 1977.

3. A. DRESCHER, R. L. MICHAŁOWSKI, *Density variation in pseudo-steady plastic flow of granular media*, Geotechnique **34**, 1, 1-10, 1984.

4. S. ICHIBA, K. HYODO, Y. OOISHI, *A study on the mechanical behavior of soil during flat edge cutting*, Mitsubishi Technical Bulletin, No. 176, 1987.

5. V. SHARMA, G. SINGH, D. GEE-CLOUGH, *Soil-tool interaction in sand*, Proc. of the 10th International Conference of the ISTVS, Kobe 1990.

6. Z. MRÓZ, J. MACIEJEWSKI, *Post-critical response of soils and shear band evolution*, CHAMBON, DERUES, VARDOULAKIS [Eds.], *Localisation and Bifurcation Theory for Soils and Rocks*, Proceedings of the 3rd International Workshop, Grenoble (Aussois), France, 6-9 September 1993, p. 19-32, Balkema 1994.

7. A. JARZĘBOWSKI, J. MACIEJEWSKI, D. SZYBA, W. TRĄMPCZYŃSKI, *Experimental and theoretical analysis of a cohesive soil shoving process (the optimization of the process), proceedings*, 6th European ISTVS Conference, (Wien, Austria) 28-30.09.1994.

8. A. JARZĘBOWSKI, J. MACIEJEWSKI, D. SZYBA, W. TRĄMPCZYŃSKI, *On the energetically most efficient trajectories for heavy machine shoving process*, Engineering Transactions, **43**, 1-2, 169-182, 1995.

9. A. JARZĘBOWSKI, J. MACIEJEWSKI, D. SZYBA, W. TRĄMPCZYŃSKI, *The optimization of heavy machines tools filling process and tools shapes (modelling test results)*, Symposium ISARC 1995, Automation and Robotics in Construction XII, E. BUDNY, A. MCCREA, K. SZYMAŃSKI [Eds.], ImBiGS 159-166, 1995.

10. L. PŁONECKI, W. TRĄMPCZYŃSKI, W. GIERULSKI, J. CENDROWICZ, K. SOKOŁOWSKI, *Computer control system for heavy machine fixtures motion and its application for automatic generation of cutting tools trajectories according to the given criteria*, Engineering Transactions, **48**, 1, 3-24, 2000.

11. W. HERMAWAN, M. YAMAZAKI, A. OIDA, *Theoretical analysis of soil reaction on a lug of the movable lug cage wheel*, Journal of Terramechanics **37**, 65-86, 2000.

Received October 11, 2000.